

# PROCEEDINGS OF SPIE

[SPIDigitalLibrary.org/conference-proceedings-of-spie](https://SPIDigitalLibrary.org/conference-proceedings-of-spie)

## Comparison between optical coherence tomography and phase shifting profilometry for surface estimation

José Gutiérrez-Gutiérrez, Verónica Mieites, Arturo Pardo, José López-Higuera, Olga Conde

José A. Gutiérrez-Gutiérrez, Verónica Mieites, Arturo Pardo, José M. López-Higuera, Olga M. Conde, "Comparison between optical coherence tomography and phase shifting profilometry for surface estimation," Proc. SPIE 12627, Translational Biophotonics: Diagnostics and Therapeutics III, 126271P (11 August 2023); doi: 10.1117/12.2670564

**SPIE.**

Event: European Conferences on Biomedical Optics, 2023, Munich, Germany

# Comparison between Optical Coherence Tomography and Phase Shifting Profilometry for surface estimation

José A. Gutiérrez-Gutiérrez<sup>1</sup>, Verónica Mieites<sup>1,2</sup>, Arturo Pardo<sup>1</sup>, José M. López-Higuera<sup>1,2,3</sup>,  
and Olga M. Conde<sup>1,2,3</sup>

<sup>1</sup>Grupo de Ingeniería Fotónica, Dep. TEISA, Universidad de Cantabria (Avda. Los Castros S/N, 39006, Santander, Spain)

<sup>2</sup>Instituto de Investigación Sanitaria Valdecilla (IDIVAL) (C. Cardenal Herrera Oria, 39011, Santander, Spain)

<sup>3</sup>CIBER-BBN (C. de Melchor Fernández Almagarro, 3, 28029, Madrid, Spain)

## ABSTRACT

Profilometry is the technique that estimates the surface height and tomography of a sample. This technique is crucial to correct the intensity variations and angle changes when optical properties of a sample are estimated and its calculation depends on the surface profile. Two systems have been evaluated in this work: an Optical Coherence Tomography (OCT) system and a Spatial-Frequency Domain Imaging (Hyperspectral-SFDI) system made up of a rotating mirror hyperspectral camera and a Red-Green-Blue (RGB) projector. The estimation of the height map with the OCT system based on the high contrasted backscattering of the air-sample interface whereas, while with the HSI-SFDI system the Phase Shifting Profilometry (PSP) technique has been implemented employing different frequencies. This work compares both approaches and evaluates the differences between them.

**Keywords:** SFDI, OCT, PSP, Hyperspectral, height map, surface profile, profilometry

## 1. INTRODUCTION

Profilometry using structured light has been a well-established technique for many years.<sup>1,2</sup> Calculating the height map of a biological sample allows for corrections to be made after the measuring stage, which is necessary in techniques such as Spatial-Frequency Domain Imaging (SFDI) or HyperSpectral Imaging (HSI).<sup>3</sup> However, profilometry methods suffer several complications and limitations when the target surface presents illumination shadows or is very absorbent.<sup>4</sup> This manuscript compares profiles obtained with Phase Shifting Profilometry (PSP), one of the most commonly used methods with structured light devices<sup>5</sup> and surface topographies obtained with Optical Coherence Tomography (OCT) providing an in depth analysis of their limitations and virtues.

The PSP technique consists of projecting a one-dimensional cosine at a certain spatial frequency onto a surface<sup>1,2</sup> and measuring the phase shift that appears which can be, for example, the surface of the optical table. This phase shift is used to estimate the height of the studied object. OCT uses a low coherence laser source to create a three-dimensional tomographic image of a sample based on the interference of the light of a reference arm and the light backscattered from the sample.<sup>6</sup> Obtaining a height map with OCT is straightforward and precise, since the highest measured intensity will be at the surface of the sample, due to the enhanced increment in backscattering caused by the refractive index mismatch between air and sample.<sup>7,8</sup>

OCT topographic maps are used as a reference to evaluate the performance of the PSP methods in terms of overall sample height, maximum height resolution and accuracy, given that our OCT system provides highly-reproducible surface maps with high spatial and axial resolution.

---

Further author information: (Send correspondence to J.A.G.G.)

J.A.G.G.: E-mail: gutierrja@unican.es

O.C.P.: E-mail: olga.conde@unican.es

## 2. MATERIALS AND METHODS

**Instrumentation.** A hyperspectral camera based on a custom mirror rotative equipment<sup>9</sup> has been used for this work. It consists of a sCMOS camera PCO Edge 4.2 (Excelitas PCO GmbH, Germany), a diffractive optics Inspector V10E (Specim, Spectral Imaging Ltd., Finland), an actuator module with a motorized rotating mirror and a RGB projector LighCrafter™4500 (1280x800) (Texas Instruments Inc., TX, USA). The OCT system is the commercial equipment TEL221PS (Thorlabs Inc., NJ, USA) has been used. This device has a central wavelength of  $\lambda = 1300nm$  and provides a  $5.5\mu m/px$  axial resolution and a field of view of  $10x10mm^2$ .

**3D calibration pieces.** As a calibration sample, a hemispheric piece has been 3D printing. Red PLA filament has been used to 3D print the pieces with a Prusa P3Steel, with 0.2 mm of tolerance, which has a minimum layer thickness of 0.2mm. The printed piece was sanded but no paint has been applied to evaluate the effects of the possible Signal to Noise Ratio (SNR) decay in darker or different colored regions within the sample. Due to limited field of view ( $10x10mm^2$ ) of the OCT, the total radius of the hemisphere has been set to 3.25mm favouring a one-to-one comparison could be made between OCT and PSP maps.

**PSP** To carry out the PSP technique, fringes based on a cosine given by  $I(x, y, f, \varphi) = I_{dc}(x, y) + M_{ac}(x, y) \cdot \cos(2\pi f + \varphi)$  have been projected where  $f$  is the spatial frequency and  $\varphi$  is the phase of the cosine. Three different  $f$  values were used ( $0.05 mm^{-1}$ ,  $0.1 mm^{-1}$ ,  $0.15 mm^{-1}$ ) and, for each frequency three  $\varphi$  values ( $240^\circ$ ,  $0^\circ$ ,  $120^\circ$ ) were projected. According with<sup>10,11</sup> the phase difference caused by the sample  $\phi'$ , can be estimated as

$$\phi'(x, y, f) = atan\left(\sqrt{3} \frac{I(x, y, f, 240^\circ) - I(x, y, f, 120^\circ)}{2I(x, y, f, 0^\circ) - I(x, y, f, 240^\circ) - I(x, y, f, 120^\circ)}\right), \quad (1)$$

where  $I$  is the image intensity captured for the pair  $(f, \varphi)$ , with  $(x, y)$  represent the spatial position of a pixel in the image. Note that  $\phi' \in [-\pi, \pi]$ <sup>12</sup> and the method requires a phase difference to estimate height of the sample. The unrolling or unwrapping method<sup>12</sup> is then applied as processing technique on  $\phi'$ . The conventional unrolling process can cause errors due to unwanted shadows or highlights. To mitigate these problems, the implementation proposed by Ghiglia et al<sup>13</sup> has been used which is based on fast transforms and iterative methods. In order to co-register the height with the phase, a phase reference  $\phi_0$  and a height reference  $h_0$  are necessary, which, if possible, should be measured below than the main surface (for example, the simplest reference can be the table or base under the sample). There are techniques in which the phase can be directly related to the height, making geometric calculations.<sup>11</sup> For the computation of the phase difference in PSP,  $\phi - \phi_0$ , a geometric analysis is required<sup>12,14</sup> but it is possible to simplify it as

$$h - h_0 = \frac{\eta}{f}(\phi - \phi_0) \quad (2)$$

where  $\eta$  is a constant ( $rad^{-1}$ ) that relates phase and frequency to height.<sup>10</sup> As mentioned before,  $f$  is the spatial frequency of the pattern in  $mm^{-1}$ ,  $h$  is the height of the surface in  $mm$ ,  $h_0$  is the reference height,  $\phi$  is the phase of the surface as given by Equation 1 and 2 and  $\phi_0$  is the reference phase. An interesting discussion would be about an analytical solution of the value of  $\eta$ , however in this manuscript  $\eta$  will be taken as a calibration constant that it is obtained through the already known dimensions of our 3D printed pieces, validated with the OCT measurements. It must be taken into account that there is a limitation of the height to be measured depending on the chosen frequency such that  $-\pi > \frac{f}{\eta}(h - h_0) > \pi$  because higher heights would cause to skip to the next cycle of the periodic function, causing errors in posterior height estimations.<sup>12</sup>

**OCT.** As mentioned before, OCT allows to obtain the tomography of a sample.<sup>15</sup> The intensity of light decreases exponentially with depth when penetrating a turbid medium. In most cases, the maximum intensity is found in the interface between the air and the surface through  $h(x, y) = \zeta \cdot argmax_z(I(x, y))$  where  $\zeta$  is the axial resolution of the laser ( $mm/px$ ),  $h$  is the height ( $mm$ ) of the sample and  $argmax_z()$  indicates the position of the maximum intensity value in the  $z$  (depth) dimension, for every  $(x, y)$  pixel in the scan.

### 3. RESULTS AND CONCLUSIONS

Figure 1 shows a comparison of the height maps obtained with PSP and OCT techniques. The relative error between both maps (Figure 1, right) is as low as than 5%, with an average of 7.23%, a median of 3% and a standard deviation of 0.1369. Areas with higher errors correspond to the lateral shadows casted by the hemisphere. Height maps obtained at various frequencies provide similar results. However, frequencies over  $0.2 \text{ mm}^{-1}$  exhibit increased errors because they became more susceptible to jumps, shadows and noise. The measurement and verification of this piece allowed us to extract the value of  $\eta$  as  $0.18 \text{ mm}^{-2}$ . This value has been obtained by measuring the phase difference  $\Delta\phi$  with a frequency of  $0.1 \text{ mm}^{-1}$  on the base of the piece, and relate it to the known height of the base (1.375 mm). This constant is the one that has been used in a measurement of a mouse muscle, to obtain the height map with PSP and OCT.

Due to the fact that the muscle is more absorbent, a height map has been obtained for each color channel (red, green and blue), at the chosen three spatial frequencies ( $0.05 \text{ mm}^{-1}$ ,  $0.1 \text{ mm}^{-1}$ ,  $0.15 \text{ mm}^{-1}$ ). It has been observed that the height varies depending on the color and the frequency. Taking the OCT measurement as a reference, it has been observed that the height map that most resembles the OCT one corresponds to the blue channel at  $0.1 \text{ mm}^{-1}$ . The reason that makes the height map change as a function of height and color would be interesting to study, but it is possible that one of the reasons is that the muscle is more absorbent in red than in green or blue, and that causes greater errors when calculating the height.

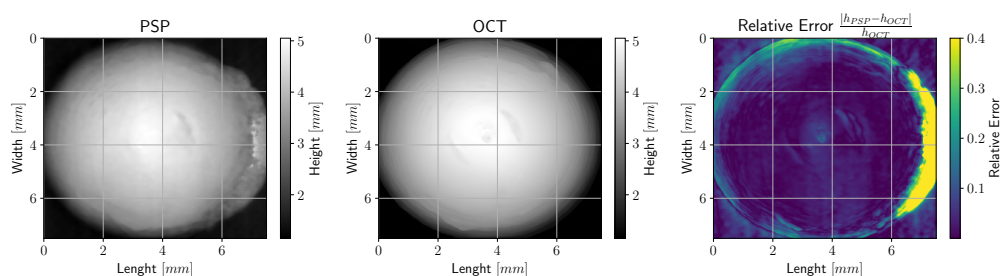


Figure 1. Topographic map obtained with PSP (left), OCT (middle) and the relative error (right) between them. It is possible to see an increased error on the rightmost regions caused by the shadow the hemisphere projects on the plane, a limitation of the PSP technique when an angled projector is used.

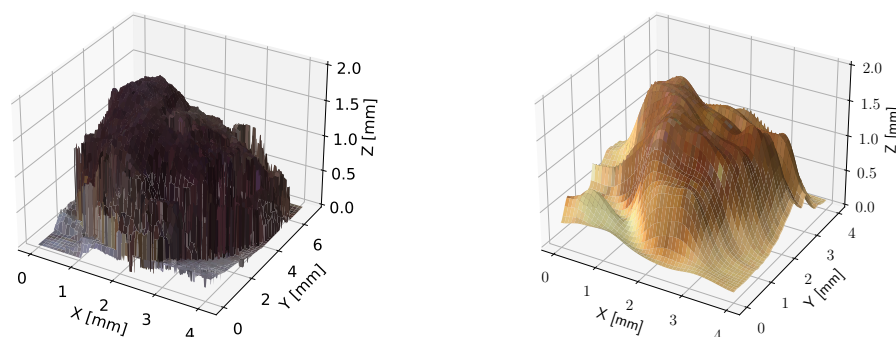


Figure 2. Comparison between the 3D surface obtained with OCT (left) and that obtained with PSP using blue channel and a frequency of  $0.1 \text{ mm}^{-1}$  (right). The RGB image of the muscle has been placed on the surface in both cases.

Figure 2 shows a 3D comparison of the muscle surface obtained in OCT and the surface obtained in PSP using the projector blue channel at a frequency of  $0.1 \text{ mm}^{-1}$ . The height map obtained with PSP has been post-processed with a Gaussian filter ( $\sigma = 16$ ) to smooth it out, since it was very noisy. Comparing both measurements is not trivial, since there is no a clear reference point. However, the maximum muscle height

measured by the PSP was 1.89 mm (in  $0.1 \text{ mm}^{-1}$ , blue channel and after filtered) while, with OCT, we calculated 1.92 mm, which would mean a relative error of 1.56% between both measurements.

The differences between the surface topographies obtained by OCT and PSP are not high therefore both methods can be used to perform a profilometry. However, it must be taken into account that when co-registering the height map with an SFDI measurement, it is much more practical to use PSP since the same system is used to do it and co-registration between measurements is immediate.

## ACKNOWLEDGMENTS

Support for this work was provided by the projects PREVAL 21/07 (FUSIOMUSCLE), SUBVTC-2021-0038 (HYPERfusionTRANS), EQC 2019-006589-P, DTS22/00127 (hyPERfusioCAM), DTS17-00055 (INTRACARDIO) and DISFOS (PID2019-107270RB-C21 /AEI/10.13039/501100011033), financed by the ISCIII, the Fundación Instituto de Investigación Valdecilla (IDIVAL) and the Spanish Ministry of Science, Innovation and Universities, co-financed with FEDER funds.

## REFERENCES

- [1] Srinivasan, V., Liu, H. C., and Halioua, M., “Automated phase-measuring profilometry of 3-D diffuse objects,” **23**(18), 3105–3108 (1984).
- [2] Srinivasan, V., Liu, H. C., and Halioua, M., “Automated phase-measuring profilometry: A phase mapping approach,” **24**(2), 185 (1985).
- [3] Gioux, S., Mazhar, A., Cuccia, D. J., Durkin, A. J., Tromberg, B. J., and Frangioni, J. V., “Three-dimensional surface profile intensity correction for spatially modulated imaging,” **14**(3), 034045 (2009).
- [4] Padilla, M., Servín, M., and Garnica, G., “Profilometry with digital Fringe-projection at the spatial and temporal Nyquist frequencies,” **25** (2017).
- [5] van de Giessen, M., Angelo, J. P., and Gioux, S., “Real-time, profile-corrected single snapshot imaging of optical properties,” **6**(10), 4051 (2015).
- [6] Huang, D., Swanson, E. A., Lin, C. P., Schuman, J. S., Stinson, W. G., Chang, W., Hee, M. R., Flotte, T., Gregory, K., Puliafito, C. A., and Fujimoto, J. G., “Optical Coherence Tomography,” **254**(5035), 1178–1181 (1991).
- [7] van Leeuwen, T., Faber, D., and Aalders, M., “Measurement of the axial point spread function in scattering media using single-mode fiber-based optical coherence tomography,” **9**(2), 227–233 (2003).
- [8] Klyen, B. R., Scolaro, L., Shavlakadze, T., Grounds, M. D., and Sampson, D. D., “Optical coherence tomography can assess skeletal muscle tissue from mouse models of muscular dystrophy by parametric imaging of the attenuation coefficient,” **5**(4), 1217 (2014).
- [9] Gutiérrez-Gutiérrez, J. A., Pardo, A., Real, E., López-Higuera, J. M., and Conde, O. M., “Custom scanning hyperspectral imaging system for biomedical applications: Modeling, benchmarking, and specifications,” **19**(7) (2019).
- [10] Geng, J., “Structured-light 3D surface imaging: A tutorial,” **3**(2), 128 (2011).
- [11] Zhou, W.-S. and Su, X.-Y., “A Direct Mapping Algorithm for Phase-measuring Profilometry,” **41**(1), 89–94 (1994).
- [12] Indebetouw, G., “Profile measurement using projection of running fringes,” **17**(18), 2930–2933 (1978).
- [13] Ghiglia, D. C. and Romero, L. A., “Robust two-dimensional weighted and unweighted phase unwrapping that uses fast transforms and iterative methods,” **11**(1), 107–117 (1994).
- [14] Sagan, H., [*Space-Filling Curves*], Springer New York, NY, 1 ed. (1994).
- [15] Kang Zhang, Weichao Wang, Jaeho Han, and Kang, J., “A Surface Topology and Motion Compensation System for Microsurgery Guidance and Intervention Based on Common-Path Optical Coherence Tomography,” **56**(9), 2318–2321 (2009).